POLITECNICO DI TORINO
Repository ISTITUZIONALE

The fabrication of Schottky photodiode by monolayer graphene direct-transfer-on-silicon

Original
The fabrication of Schottky photodiode by monolayer graphene direct-transfer-on-silicon / Wang, Yiming; Yang, Shuming; Ballesio, Alberto; Parmeggiani, Matteo; Verna, Alessio; Cocuzza, Matteo; Pirri, Candido Fabrizio; Marasso, Simone Luigi. - In: JOURNAL OF APPLIED PHYSICS. - ISSN 0021-8979. - ELETTRONICO. - 128:1(2020), p. 014501. [10.1063/5.0004242]

Availability:
This version is available at: 11583/2837982 since: 2020-07-02T09:42:30Z

Publisher:
AIP Publishing

Published
DOI:10.1063/5.0004242

Terms of use:

This article is made available under terms and conditions as specified in the corresponding bibliographic description in the repository

Publisher copyright
AIP postprint/Author's Accepted Manuscript e postprint versione editoriale/Version of Record

(Article begins on next page)

14 November 2024

Journal of
Applied Physics

The fabrication of Schottky photodiode by monolayer graphene direct-transfer-on-silicon

Cite as: J. Appl. Phys. **128**, 014501 (2020); https://doi.org/10.1063/5.0004242
Submitted: 09 February 2020 . Accepted: 16 June 2020 . Published Online: 01 July 2020

Yiming Wang, Shuming Yang, Alberto Ballesio, Matteo Parmeggiani, Alessio Verna, Matteo Cocuzza, Candido Fabrizio Pirri, and Simone Luigi Marasso

Lock-in Amplifiers
up to 600 MHz

© 2020 Author(s).

Journal of Applied Physics ARTICLE scitation.org/journal/jap

The fabrication of Schottky photodiode by monolayer graphene direct-transfer-on-silicon

Cite as: J. Appl. Phys. **128**, 014501 (2020); doi: 10.1063/5.0004242
Submitted: 9 February 2020 · Accepted: 16 June 2020 ·
Published Online: 1 July 2020

View Online

Export Citation

CrossMark

Yiming Wang,[1,2] Shuming Yang,[1,a)] Alberto Ballesio,[2] Matteo Parmeggiani,[2,3] Alessio Verna,[2] Matteo Cocuzza,[2,4] Candido Fabrizio Pirri,[2,3] and Simone Luigi Marasso[2,4]

AFFILIATIONS

[1]State Key Laboratory for Manufacturing System Engineering, Xi'an Jiaotong University, Xi'an, Shaanxi 710049, China
[2]Chilab—Materials and Microsystems Laboratory, DISAT, Politecnico di Torino—Via Lungo Piazza, d'Armi 6, IT 10034, Chivasso (Turin), Italy
[3]Center for Sustainable Future Technologies, Italian Institute of Technology, Corso Trento 21, IT 10129 Turin, Italy
[4]CNR-IMEM, Parco Area delle Scienze 37a, IT 43124, Parma, Italy

[a)]**Author to whom correspondence should be addressed:** shuming.yang@mail.xjtu.edu.cn

ABSTRACT

A two-step hot embossing process was used to transfer graphene and to fabricate Gr/Si Schottky photodiodes. As a direct graphene transfer technique through a hot embossing system, chemical vapor deposition Gr monolayer was transferred from copper foil to cyclic olefin copolymer foil without a poly(methylmethacrylate) sacrificial layer. Then, hot embossing was employed once again to bond graphene with the prepared Si substrate to form Schottky contact. Electrical and photoelectrical characterizations have been performed to evaluate the Schottky photodiode. The photocurrent increases linearly with light intensity under 633 nm illumination. With an appropriate bias voltage, the maximum responsivity reaches 0.73 A/W. Extracted from I–V characteristics by Cheung's function, the Schottky barrier height and ideality factor are 1.01 eV and 2.66, respectively. The experimental result shows the feasibility and effectiveness of this hot embossing fabrication process, which demonstrates the opportunity for large scale production and provides a new approach for graphene optoelectronics.

Published under license by AIP Publishing. https://doi.org/10.1063/5.0004242

I. INTRODUCTION

Graphene photodetectors have experienced rapid development in the past decade, owing to the unique electrical and optical properties of graphene such as high charge carrier mobility and wide spectrum light absorption.[1] As we know, graphene, the first truly two-dimensional material,[2] was successfully obtained by the mechanical exfoliation method, which is lowly efficient and not suitable for mass production.[3] Since then, much effort has been devoted to the effective synthesis of high-quality graphene.[4–7] From the developing trends over recent years,[8] chemical vapor deposition (CVD) is the most promising among all other methods to obtain monolayers for integration in large scale device production. However, the CVD growth needs a metal seed layer like Cu and Ni and, hence, graphene transfer technologies became the key point between synthesis and application.[9–12] The most frequently used graphene transfer method is based on a polymethylmethacrylate (PMMA) sacrificial layer and metal etching processes, but it suffers from the residues of PMMA and it is hard to scale to a large area and match the semiconductor manufacturing compatibility.

Graphene/silicon (Gr/Si) Schottky junction is one of the most important components of graphene based photosensitive devices. In Gr/Si Schottky photodiodes, the incident light passes through the graphene layer and the photons are absorbed by silicon to excite electron–hole pairs. During this process, graphene collects the photo-generated carriers and provides a high speed pathway for carrier transport.[1] Since Li *et al.* transferred the CVD graphene on an HF etched n-type Si wafer,[13] Gr/Si photoelectrical devices has attracted great attention.[14–17]

The most frequently used method to fabricate Gr/Si Schottky devices uses PMMA as a sacrificial media layer to transfer graphene from the original metal substrate to the silicon substrate.[17–21] In this traditional method, PMMA solution with a certain concentration is spin-coated on the graphene/metal substrate and heated to evaporate the solvent to form a PMMA layer. After etching the

Published under license by AIP Publishing.

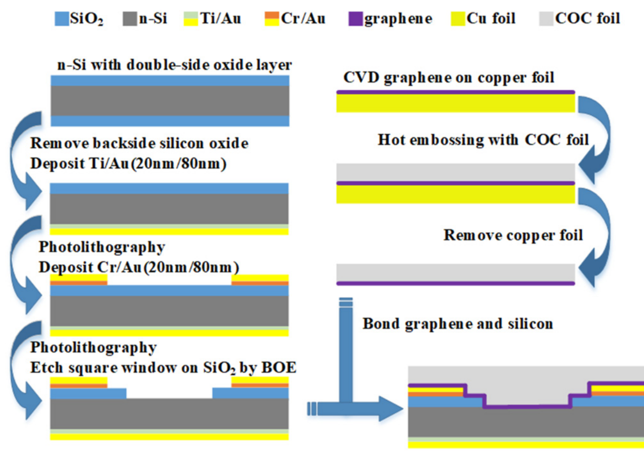

FIG. 1. Fabrication process of hot embossing transferred Gr/Si Schottky photodiode.

metal substrate by copper etching solution [usually $FeCl_3$, sometimes $(NH_4)_2S_2O_8$], the PMMA/graphene floating over the air–liquid interface is picked up by silicon substrate and form Gr/Si Schottky contact. However, it is a manual procedure to pick up graphene from the liquid surface to the desired substrate, which cannot match the semiconductor manufacturing compatibility and, on the other hand, causes wrinkles and folds of graphene films in the handcraft. As a sacrificial media, PMMA should be removed after graphene transferring, but the PMMA residue is a major problem exercising the minds of scientists around the world. The residues trap the photogenerated charge carriers when they move through the interface, causing an increase in electron/hole

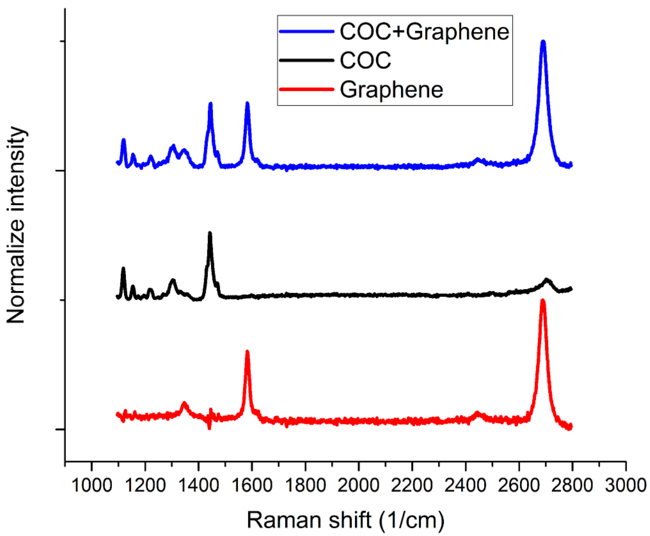

FIG. 2. Raman spectrum of hot embossing transferred graphene.

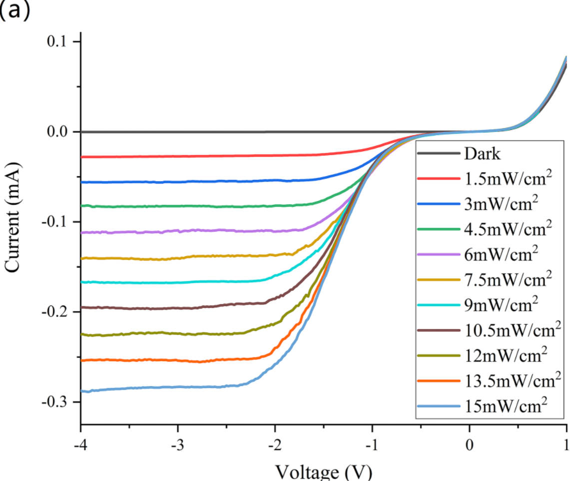

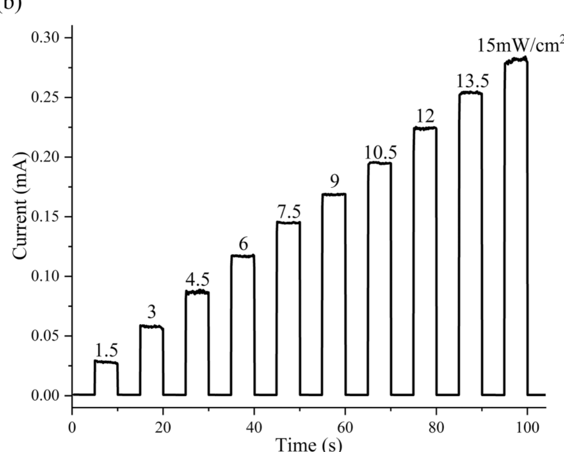

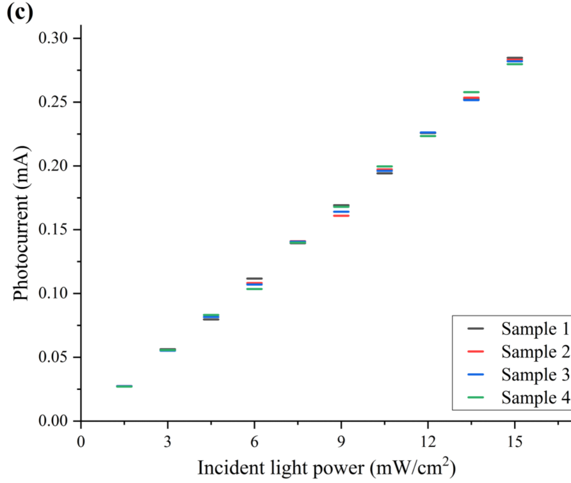

FIG. 3. (a) Current–voltage curve of Gr/n-Si Schottky photodiode under various incident light powers. (b) Time dependent photocurrent response. (c) Photocurrent of different samples under various incident light power.

Published under license by AIP Publishing.

recombination and the degradation of device performance.[17] To solve this problem, deep UV treatment,[18,19] Ar ion beam,[20] low molecular weight PMMA,[21] etc. were used to reduce the PMMA residues, while the processes became more complicated.

Hot embossing is a cost-effective and flexible fabrication technology which has been widely used for micro-/nano-fabrication, but it has been used only recently to transfer CVD grown graphene.[22] By applying this novel method, CVD grown graphene was successfully transferred from copper foil to cyclic olefin copolymer (COC) foil without the PMMA sacrificial layer. The hot embossing process avoids the residues of PMMA and simplifies the processing steps, thus providing the opportunity for large scale production. As a widely used technique, hot embossing has good processing compatibility to micro-/nano-manufacturing and it does not require careful operation, which is a significant advantage of this method compared with other PMMA-free graphene method.[11,23,24] The success of hot embossing graphene is the transferring benefits from the nature of the polymer material, which is flexible and able to contact well with graphene on the original metal substrate under certain pressure and temperature. As a result, this method was mainly used to fabricate flexible graphene devices, while at present, there is no attempt on the graphene device on a hard substrate by this method.

In this work, the hot embossing process was employed twice to transfer graphene and fabricate Gr/Si Schottky photodiodes. As a direct graphene transfer technique, CVD monolayer graphene was transferred by hot embossing from copper foil to COC foil without the PMMA sacrificial layer.[22] The SiO_2/Si substrate with a square window oxide layer and front and backside electrodes was prepared by photolithography, e-beam evaporation, and wet etching. Then, hot embossing was employed once again to bond graphene/COC with the as-prepared substrate from Schottky contact in the window of an insulating layer. Considering the good high transparency of the COC material, the COC foil remains on the top of photodiode and protects graphene from external pollution. The incident light goes through transparent COC and graphene layer, and finally excites electron–hole pairs in silicon, which is the origin of photoelectrical response of Gr/Si Schottky diodes. This paper demonstrates this new strategy to fabricate Gr/Si Schottky photodiodes. We also investigate the photo-response using a 633 nm laser at different intensities and evaluate the relevant parameters using the thermionic emission model and Cheung's method, which reveals that the Gr/Si Schottky diode fabricated by hot embossing has the equivalent or even better performance as those fabricated by the traditional method.

II. EXPERIMENTAL

A. Graphene growth and transferring to COC

After rinsing Cu foils in 10% HCl for 15 min, the single layer graphene was grown on them in a CVD system (Moorfield NanoCVD 8G). Gr/Cu was then hot embossed onto a COC foil (140 μm, TOPAS 8007 × 04). This process was performed with a hot embossing system (model HEX01JENOPTIK Mikrotechnik) with the temperature of 80 °C and the applied force of 10 000 N for 120 s. Since the surface was $2 \times 2\ cm^2$, the pressure was 25 MPa. Then the Cu layer was wet etched by $FeCl_3$ solution and the samples were rinsed in de-ionized (DI) water to remove $FeCl_3$ residues, thus graphene on COC was obtained.

B. Fabrication of Gr/Si Schottky photodiode

n-type Si (100) wafer (1–10 Ω cm) with 300 nm SiO_2 was used as the substrate for the fabrication of Schottky junction. First, the SiO_2 layer on the backside was removed by HF etching, and Ti/Au (20 nm/80 nm) was deposited by e-beam evaporation to form ohmic contact. After that, the Cr/Au (20 nm/80 nm) electrode was patterned and evaporated on the front side of the SiO_2/Si wafer.

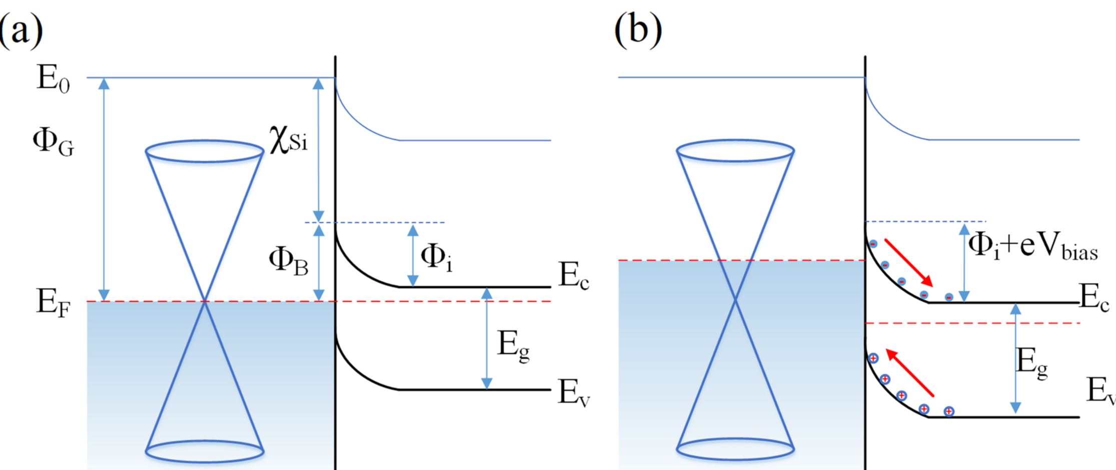

FIG. 4. Energy band diagram of the Gr/Si Schottky junction. (a) Thermal equilibrium energy band diagram of the heterojunction in darkness. (b) Reverse bias under illumination. E_c, E_v, E_F, E_g, Φ_G, χ_{Si}, Φ_B, and Φ_i denote conduction band, valence band, Fermi level, bandgap, work function of graphene, electron affinity of silicon and Schottky barrier height, built-in potential, respectively.

Published under license by AIP Publishing.

Photolithography was used to define a square window on the substrate ($1.6 \times 1.6\,mm^2$), followed by a wet etching process in buffered oxide etch (BOE) solution to remove the SiO_2 layer. Then, hot embossing was used once again to bond graphene with the prepared silicon substrate to form Schottky contact in the window, which was the active area of this photodetector.

C. Raman, electrical, and photoelectrical characterizations

Raman microscope (Renishaw plc, Wotton-under-Edge, UK) with a 532 nm laser and a Leica DMLM microscope were used to characterize graphene transferred by the hot embossing process. The spectrum of the COC foil was obtained in advance and was taken off from that of graphene on COC to get the contribution of graphene alone.

Keysight B2912A Source/Measure unit was used for electrical characterizations, and photoelectrical characterization was carried out under dark and 633 nm illumination with a semiconductor laser (laser power has been calibrated with Sanwa LP-1 before the measurements). Based on the thermionic emission theory, the ideality factor and Schottky barrier height were extracted from the current–voltage curve to evaluate the property of Gr/Si Schottky diodes.

III. RESULTS AND DISCUSSION

The Raman spectrum of graphene transferred on the COC foil by hot embossing (Figs. 1 and 2) shows three main peaks: D peak at $1346\,cm^{-1}$, G peak at $1582\,cm^{-1}$, and 2D peak at $2678\,cm^{-1}$. The 2D peak is sharp and symmetric, the full width at half maximum of the 2D peak is $35\,cm^{-1}$, and the intensity ratio of the 2D peak to the G peak is 1.75. The shape of the peaks and the intensity ratio indicate the monolayer nature of this graphene thin film.[25–27] From the Raman spectrum, it can be seen that the graphene structure is well preserved after experiencing the 25 MPa molding pressure during the hot embossing process.

As shown in Fig. 3(a), I–V measurements were carried out under different incident light intensities from 0 to $15\,mW/cm^2$. The curves exhibit typical rectifying behavior and Gr/Si Schottky junction works in the backward voltage segment, which is similar to that of a metal/semiconductor Schottky diode. From the family of I−V curves, we can see that the photocurrent of the device is highly dependent on the bias voltage: for a certain incident light power, the photocurrent rises with the increase in reverse bias and saturates at higher reverse bias. This phenomenon originates for the photovoltaic characteristic of the Gr/Si Schottky junction, which can be understood from the energy band diagram as shown in Fig. 4. At the graphene/silicon interface, the incident photons are absorbed by silicon and excite electron–hole pairs, which are separated by the built-in potential and transported efficiently to the external electrode under the appropriate biases, where graphene acts as a carrier collector and a high-speed channel for photogenerated carriers. While the built-in potential, Φ_i, is related to the bias voltage, as shown in Fig. 4(b), the ability of charge separation can be tuned by the bias and a relatively large built-in potential is favorable for injecting all of the photoexcited holes from silicon to graphene and obtaining the saturated photocurrent.

While an appropriate reverse bias is applied on the Gr/Si Schottky junction, the saturated photocurrent increases linearly with the incident light intensity. Figure 3(b) displays the time dependent photoresponse to a pulse optical signal of various intensities with the reverse bias voltage of −3 V, which shows the reliability and stability of the hot embossing fabricated Gr/Si photodiode. The responsivity of the hot embossing Gr/n-Si Schottky photodiode was measured to be 0.73 A/W. Four samples have been fabricated using the same processes, and their photoresponses were measured under various incident light powers with a reverse bias voltage of 3 V. As shown in Fig. 3(c), their photocurrents are almost same under the same incident light power, which indicates the stability and reliability of the two-step hot embossing process.

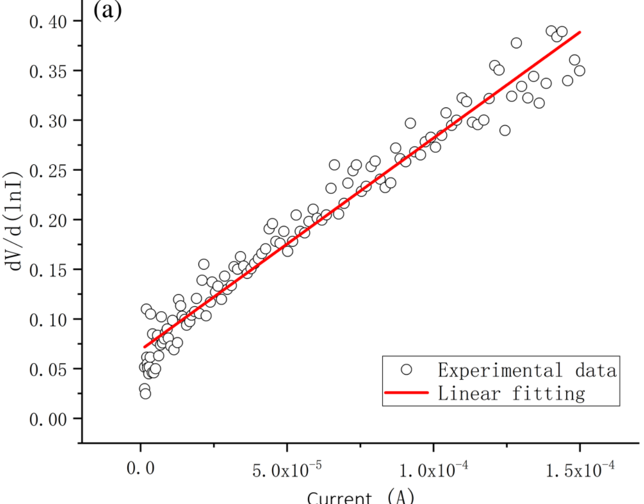

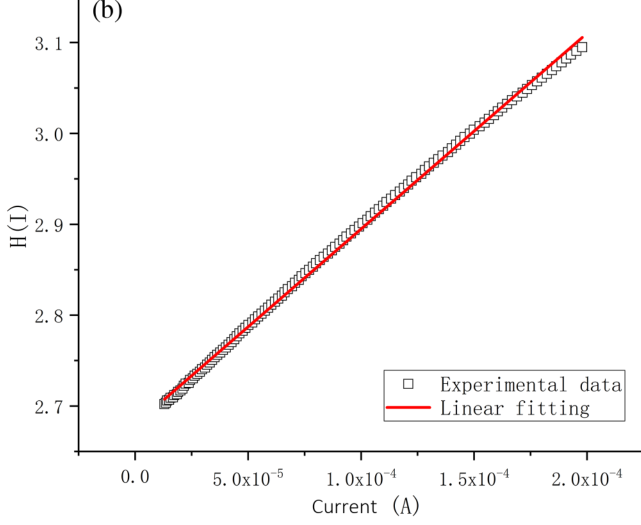

FIG. 5. Plots of dV/d(ln I) vs I (a), and H(I) vs I (b) for the Gr/Si Schottky diode.

Published under license by AIP Publishing.

TABLE I. Summary of the performances of the graphene based photodetectors.

Device structure	Responsivity (A/W)	Schottky barrier height (eV)	Series resistance (Ω)	Ideality factor	Reference
Graphene/Si	0.73	1.01	∼2100	2.66	This work
Graphene/Si	0.73	…	…	…	1
Graphene/Si	0.23	0.66	6700	1.52	30
Graphene/Si	0.435	…	…	…	31
Graphene/Si	0.140	0.79	32.1	2.24	14
Graphene/Si	0.214	0.79	…	2.1	15
Graphene/Si	0.152	…	…	…	16
Graphene/Si	0.142	0.79	14.9	…	17
Graphene/Si	0.24	…	…	…	32
Gr/Si-tips junction	2.5	0.36	4500	…	33
PEDOT-graphene/Si	0.172	…	…	…	16
P3HT-graphene/Si	0.78	…	…	…	32
TFSA-graphene/Si	0.252	0.89	10.3	…	17
MoO_3-graphene/Si	0.4	0.86	17.1	1.3	14
Graphene/GO/Si	0.266	0.81	…	2.6	15
Graphene/metal	0.225	…	…	…	34
Graphene/Ge	0.0518	…	…	…	35

To further investigate the hot embossing Gr/Si Schottky photodiode, the key Schottky parameters were extracted from current–voltage measurement. The current–voltage relationship of the Gr/n-Si junction can be described by the thermionic emission theory,

$$I = I_0\left(e^{\frac{qV}{\eta kT}} - 1\right), \tag{1}$$

where η is the ideality factor, I_0 is the saturation current defined by

$$I_0 = AA^* T^2 e^{-\frac{\Phi_B}{kT}}, \tag{2}$$

where A, A^*, and Φ_B are, respectively, the diode area, Richardson constant, and zero-bias barrier height. When considering the effect of series resistance (R_s), V in Eq. (1) can be replaced by the difference of the total voltage drop of the system and the voltage drop of series resistance, and two new equations can be derived from it,

$$\frac{\partial V}{\partial(\ln I)} = \frac{\eta kT}{q} + R_s I, \tag{3}$$

$$H(I) = IR_s + \eta\Phi_B, \tag{4}$$

where $H(I)$ is given by

$$H(I) = V - \eta\left(\frac{kT}{q}\right)\ln\left(\frac{I}{AA^* T^2}\right). \tag{5}$$

Accordingly, the experimental values of ideality factor η, series resistance R_s, and Schottky barrier height Φ_B can be extracted from the non-linear region of the forward bias I–V characteristics by Cheung's functions.[28,29]

Plots of $dV/d(\ln I)$ vs I and $H(I)$ vs I for the Gr/Si Schottky diode are presented in Fig. 5. From the plot of $dV/d(\ln I)$–I [Fig. 5(a)], the values of series resistance and ideality factor are determined to be 2132 Ω and 2.66 from the intercept and slope of the forward bias, respectively. Using the ideality factor value obtained from the $dV/d(\ln I)$–I plot, the Schottky barrier height is estimated by Eq. (4) from the $H(I)$–I plot [Fig. 5(b)]. Φ_B and R_s are found to be 1.01 eV and 2153 Ω, respectively. The R_s values obtained from the both plots are almost the same, which can be attributed to the consistency of Cheung's functions.[29]

Table I lists the performances of graphene based photodetectors, most of them are graphene/silicon Schottky structure, some surface modified graphene devices and graphene heterojunction with other materials are also included, it can be seen that the hot embossing fabricated Gr/Si shows the same level of photodetecting ability with the ones already published.

In a Schottky photodiode, photogenerated electron–hole pairs are separated by a built-in electric field associated with the Schottky barrier,[36–38] thus the responsivity of 0.73 A/W was obtained with the high Schottky barrier height of 1.01 eV. However, in the meantime, the series resistance reaches more than 2 kΩ, which is higher than the traditional Gr/Si photodiode fabricated by PMMA graphene transfer.[1,14] The high series resistance may attribute to the scratch or tear of graphene near to the edge of silicon window, in which a 300 nm high silicon oxide step locates. The high ideality factor also indicates that the complex interface causes a negative impact on the device performance. In spite of this, the sensitive, quick, and stable photoresponse shows the feasibility and effectiveness of this hot embossing fabrication process, which provides a new approach for graphene devices.

IV. CONCLUSION

In conclusion, a straightforward fabrication method of Gr/Si Schottky photodiode via the hot embossing process has been successfully developed. The hot embossing process was used both

Published under license by AIP Publishing.

to transfer CVD graphene from copper to COC, and to bond graphene with the Si substrate to form Schottky contact. The responsivity of this Gr/Si photodiode reaches 0.73 A/W under 633 nm illumination with a reverse bias of −3 V, which can be attributed to the high Schottky barrier height. Overall, this straightforward method allows us to fabricate graphene based devices efficiently and demonstrates the opportunity for large scale production.

ACKNOWLEDGMENTS

The present work was performed in the framework and financed by the POLITO BIOMed LAB, an interdepartmental laboratory financed by the Politecnico di Torino and DEFLeCT ("Advanced platform for the early detection of not small cells lung cancer," Piedmont "Health & WellBeing" Platform) project. DEFLeCT project was funded by the Regione Piemonte POR-FESR 2014-2020. The authors would like to acknowledge support by the National Natural Science Foundation of China (NNSFC) (No. 51575440), the National Science Fund for Excellent Young Scholars (No. 51722509), the National Key R&D Program of China (No. 2017YFB1104700), and the China Scholarship Council.

DATA AVAILABILITY

The data that support the findings of this study are available from the corresponding author upon reasonable request.

REFERENCES

[1]X. Li, M. Zhu, M. Du, Z. Lv, L. Zhang, Y. Li, Y. Yang, T. Yang, X. Li, and K. Wang, Small **12**, 595–601 (2016).
[2]X. Wang, Z. Cheng, K. Xu, H. K. Tsang, and J.-B. Xu, Nat. Photonics **7**, 888 (2013).
[3]K. S. Novoselov, A. K. Geim, S. V. Morozov, D. Jiang, M. I. Katsnelson, I. V. Grigorieva, S. V. Dubonos, and A. A. Firsov, Nature **438**, 197–200 (2005).
[4]D. Geng, H. Wang, and G. Yu, Adv. Mater. **27**, 2821–2837 (2015).
[5]D. Q. McNerny, B. Viswanath, D. Copic, F. R. Laye, C. Prohoda, A. C. Brieland-Shoultz, E. S. Polsen, N. T. Dee, V. S. Veerasamy, and A. J. Hart, Sci. Rep. **4**, 5049 (2015).
[6]A. Mohsin, L. Liu, P. Liu, W. Deng, I. N. Ivanov, G. Li, O. E. Dyck, G. Duscher, J. R. Dunlap, and K. Xiao, ACS Nano **7**, 8924–8931 (2013).
[7]F. Han, S. Yang, W. Jing, K. Jiang, Z. Jiang, H. Liu, and L. Li, Appl. Surf. Sci. **314**, 71–77 (2014).
[8]G. Deokar, J. Avila, I. Razado-Colambo, J.-L. Codron, C. Boyaval, E. Galopin, M.-C. Asensio, and D. Vignaud, Carbon **89**, 82–92 (2015).
[9]X.-D. Chen, Z.-B. Liu, C.-Y. Zheng, F. Xing, X.-Q. Yan, Y. Chen, and J.-G. Tian, Carbon **56**, 271–278 (2013).
[10]L. Gao, G.-X. Ni, Y. Liu, B. Liu, A. H. C. Neto, and K. P. Loh, Nature **505**, 190–194 (2014).
[11]G. Zhang, A. G. Güell, P. M. Kirkman, R. A. Lazenby, T. S. Miller, and P. R. Unwin, ACS Appl. Mater. Interfaces **8**, 8008–8016 (2016).
[12]Y. Fan, K. He, H. Tan, S. Speller, and J. H. Warner, Chem. Mater. **26**, 4984–4991 (2014).
[13]X. Li, H. Zhu, K. Wang, A. Cao, J. Wei, C. Li, Y. Jia, Z. Li, X. Li, and D. Wu, Adv. Mater. **22**, 2743–2748 (2010).
[14]D. Xiang, C. Han, Z. Hu, B. Lei, Y. Liu, L. Wang, W. P. Hu, and W. Chen, Small **11**, 4829–4836 (2015).
[15]L. Yang, X. Yu, M. Xu, H. Chen, and D. Yang, J. Mater. Chem. A **2**, 16877–16883 (2014).
[16]T. Feng, D. Xie, Y. Lin, H. Zhao, Y. Chen, H. Tian, T. Ren, X. Li, Z. Li, and K. Wang, Nanoscale **4**, 2130–2133 (2012).
[17]X. Miao, S. Tongay, M. K. Petterson, K. Berke, A. G. Rinzler, B. R. Appleton, and A. F. Hebard, Nano Lett. **12**, 2745–2750 (2012).
[18]M. Jang, T. Q. Trung, J.-H. Jung, B.-Y. Kim, and N.-E. Lee, Phys. Chem. Chem. Phys. **16**, 4098–4105 (2014).
[19]A. Suhail, K. Islam, B. Li, D. Jenkins, and G. Pan, Appl. Phys. Lett. **110**, 183103 (2017).
[20]K. S. Min, K. S. Kim, K. N. Kim, A. Mishra, and G. Y. Yeom, J. Nanosci. Nanotechnol. **14**, 9108–9113 (2014).
[21]S. Kim, S. Shin, T. Kim, H. Du, M. Song, C. Lee, K. Kim, S. Cho, D. H. Seo, and S. Seo, Carbon **98**, 352–357 (2016).
[22]A. Ballesio, M. Parmeggiani, A. Verna, F. Frascella, M. Cocuzza, C. F. Pirri, and S. L. Marasso, Microelectron. Eng. **209**, 16–19 (2019).
[23]W.-H. Lin, T.-H. Chen, J.-K. Chang, J.-I. Taur, Y.-Y. Lo, W.-L. Lee, C.-S. Chang, W.-B. Su, and C.-I. Wu, ACS Nano **8**, 1784–1791 (2014).
[24]S. Cha, M. Cha, S. Lee, J. H. Kang, and C. Kim, Sci. Rep. **5**, 17877 (2015).
[25]R. Liu, X.-W. Fu, J. Meng, Y.-Q. Bie, D.-P. Yu, and Z.-M. Liao, Nanoscale **5**, 5294–5298 (2013).
[26]Z. Ni, Y. Wang, T. Yu, and Z. Shen, Nano Res. **1**, 273–291 (2008).
[27]D. P. Yu, Adv. Mater. **23**, 3938–3943 (2011).
[28]S. K. Cheung and N. W. Cheung, Appl. Phys. Lett. **49**, 85–87 (1986).
[29]L. D. Rao, K. S. Latha, V. R. Reddy, and C. Choi, Vacuum **119**, 276–283 (2015).
[30]S. Riazimehr, D. Schneider, C. Yim, S. Kataria, V. Passi, A. Bablich, G. S. Duesberg, and M. C. Lemme, *Spectral Sensitivity of a Graphene/Silicon pn-Junction Photodetector* (IEEE, 2015), pp. 77–80.
[31]X. An, F. Liu, Y. J. Jung, and S. Kar, Nano Lett. **13**, 909–916 (2013).
[32]H. Aydın, S. B. Kalkan, C. Varlikli, and C. Çelebi, Nanotechnology **29**, 145502 (2018).
[33]A. Di Bartolomeo, G. Luongo, L. Iemmo, F. Urban, and F. Giubileo, IEEE Trans. Nanotechnol. **17**, 1133–1137 (2018).
[34]S. Cakmakyapan and M. Jarrahi, *High Responsivity and Bias-Free Graphene Photodetector with Nano-Grating Contact Electrodes* (OSA, 2018), pp. 1–2.
[35]L.-H. Zeng, M.-Z. Wang, H. Hu, B. Nie, Y.-Q. Yu, C.-Y. Wu, L. Wang, J.-G. Hu, C. Xie, F.-X. Liang, and L.-B. Luo, ACS Appl. Mater. Interfaces **5**, 9362–9366 (2013).
[36]X. Liu, X. W. Zhang, Z. G. Yin, J. H. Meng, H. L. Gao, L. Q. Zhang, Y. J. Zhao, and H. L. Wang, Appl. Phys. Lett. **105**, 183901 (2014).
[37]S. Shafique, S. Yang, Y. T. Woldu, and W. Yiming, Sens. Actuators A **288**, 107–116 (2019).
[38]S. Shafique, S. Yang, Y. Wang, Y. T. Woldu, B. Cheng, and P. Ji, Sens. Actuators A **296**, 38–44 (2019).

Published under license by AIP Publishing.